

HETEROCYCLES, Vol. 100, No. 10, pp. 1633 - 1644. © 2020 The Japan Institute of Heterocyclic Chemistry
Received, 17th June, 2020, Accepted, 22nd July, 2020 Published online, 20th August, 2020
DOI: 10.3987/COM-20-14305

**IDENTIFICATION AND CHARACTERIZATION OF
CHLORINE-CONTAINING BRIARANES FROM A CULTURED
OCTOCORAL *BRIAREUM EXCAVATUM* (BRIAREIDAE)**

**Yi-Lin Zhang,^{a,b†} Liang-Mou Kuo,^{c,d†} Lo-Yun Chen,^{b,e} Gene-Hsiang Lee,^f
Bo-Rong Peng,^b You-Ying Chen,^b Yu-Hsin Chen,^b Tsong-Long Hwang,^{g,h,i,j,*}
Jyh-Horng Sheu,^{k,*} and Ping-Jyun Sung^{a,b,k,l,m,*}**

^a Graduate Institute of Marine Biology, National Dong Hwa University, Pingtung 944401, Taiwan. ^b National Museum of Marine Biology and Aquarium, Pingtung 944401, Taiwan. ^c Department of General Surgery, Chang Gung Memorial Hospital at Chia-Yi, 613016, Taiwan. ^d School of Medicine, College of Medicine, Chang Gung University, Taoyuan, 333323, Taiwan. ^e Department of Chemistry, National Sun Yat-sen University, Kaohsiung 804201, Taiwan. ^f Instrumentation Center, National Taiwan University, Taipei 106319, Taiwan. ^g Research Center for Chinese Herbal Medicine, Research Center for Food and Cosmetic Safety, Graduate Institute of Healthy Industry Technology, College of Human Ecology, Chang Gung University of Science and Technology, Taoyuan 333324, Taiwan. ^h Graduate Institute of Natural Products, College of Medicine, Chang Gung University, Taoyuan 333323, Taiwan. ⁱ Chinese Herbal Medicine Research Team, Healthy Aging Research Center, Chang Gung University, Taoyuan 333323, Taiwan. ^j Department of Anaesthesiology, Chang Gung Memorial Hospital, Taoyuan 333423, Taiwan. ^k Department of Marine Biotechnology and Resources, National Sun Yat-sen University, Kaohsiung 804201, Taiwan. ^l Chinese Medicine Research and Development Center, China Medical University Hospital, Taichung 404394, Taiwan. ^m Graduate Institute of Natural Products, Kaohsiung Medical University, Kaohsiung 807378, Taiwan.

E-mail: htl@mail.cgu.edu.tw, sheu@mail.nsysu.edu.tw, pjsung@nmma.gov.tw

[†] Equal contribution to this article.

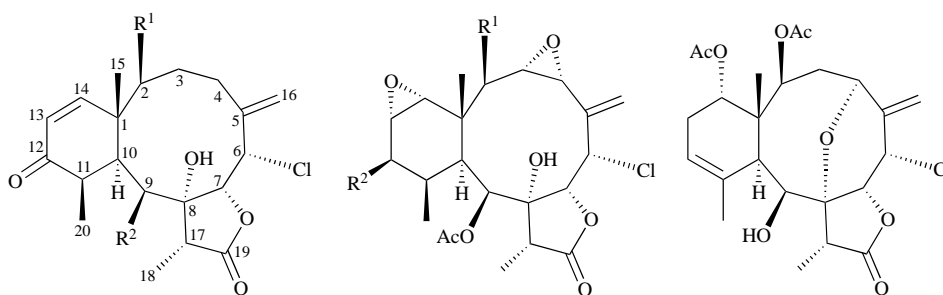
Abstract – Six chlorine-containing briaranes, including two new compounds, briarenols M (**1**) and N (**2**), as well as four known metabolites solenolide E (**3**),

briarenolide R (**4**), excavatolide A (**5**), and briaexcavatolide F (**6**), have been isolated from a cultured octocoral identified as *Briareum excavatum*. The structures of **1** and **2** were established by spectroscopic methods and the absolute configurations of **5** and **6** were confirmed by single-crystal X-ray diffraction analysis. These compounds were subjected into the inhibitory effects on fMLF/CB stimulated superoxide anion generation and elastase release in human neutrophils.

The octocoral *Briareum excavatum* (Nutting 1911, family Briareidae, order Alcyonacea, class Anthozoa, phylum Cnidaria),¹⁻⁴ were proven to be the most important flagship-species to produce briarane-type natural products,⁵ and the compounds of this type have been reported to exhibit interesting bioactivities, such as anti-inflammatory activity.⁶ Due to most of the pharmaceutical-potentially coral reef organisms are claimed to be endangered species. In order to protect natural population and habits for these target marine organisms from over exploitation and stable supporting bioactive material for further study,⁷ a cultured octocoral *B. excavatum* was studied for its chemical constituents related to briaranes (Chart 1). We reported herein the structures of six chlorine-containing briarane lactones, including two new isolates, briarenols M (**1**) and N (**2**), and four known metabolites, solenolide E (**3**),⁸ briarenolide R (**4**),⁹ excavatolide A (**5**),¹⁰⁻¹² and briaexcavatolide F (**6**)¹³ (Chart 1). The *in vitro* anti-inflammatory suppression assay of compounds **1–5** were tested for their inhibition of elastase release and superoxide anion generation from human neutrophils.



B. excavatum



- 1:** R¹ = OAc, R² = OAc
2: R¹ = OAc, R² = OCO(CH₂)₂Me
3: R¹ = OAc, R² = OH
4: R¹ = OH, R² = OH
5: R¹ = OH, R² = OCO(CH₂)₂Me
6: R¹ = OAc, R² = OCOCH₂CH(Me)₂
8: R¹ = R² = OAc

Chart 1. Picture of *B. excavatum* and the structures of briarenols M (**1**) and N (**2**), solenolide E (**3**), briarenolide R (**4**), excavatolide A (**5**), briaexcavatolide F (**6**), briaviolide E (**7**), and briaexcavatolide E (**8**)

Excavatolide A (**5**) and briaexcavatolide F (**6**) were first isolated from the octocorals belonging to the genus *Briareum*, distributed in the waters of Taiwan; and the structures of these two compounds were elucidated by spectroscopic analysis.^{10,13} The absolute configurations of **5** and **6** were determined in this study by single-crystal X-ray diffraction analyses for the first time (Flack parameter $x = 0.081(4)$ for **5**; and $x = 0.055(7)$ for **6**) and the ORTEP diagram (Figure 1) showed that the absolute configurations of stereogenic carbons of **5** are $1R,2S,4S,6S,7R,8R,9S,10S,14S,17R$ and of **6** are $1S,2R,3S,4R,6S,7R,8R,9S,10S,11R,12R,13S,14R,17R$.

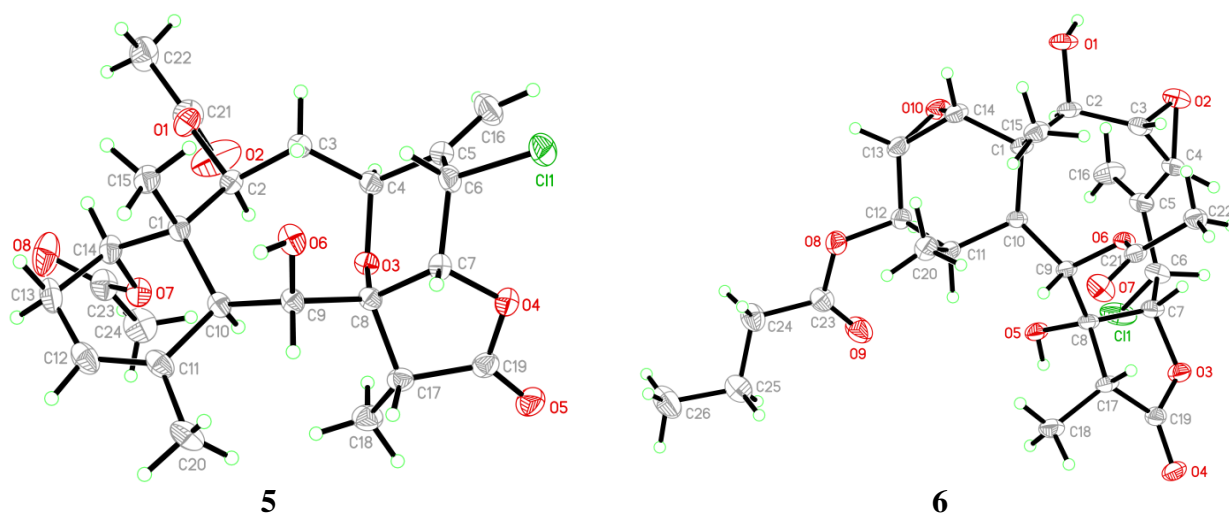


Figure 1. The computer-generated ORTEP plots of excavatolide A (**5**) and briaexcavatolide F (**6**)

Briarenol M (**1**) was obtained as an amorphous powder. The molecular formula of **1** was established as $C_{24}H_{31}ClO_8$ (unsaturation degrees = 9) from a sodiated molecule at m/z 505 in the ESIMS and was further supported by HRESIMS (m/z 505.15993, Calcd for $C_{24}H_{31}^{35}ClO_8 + Na$, 505.15997). The IR spectrum suggested the presence of hydroxy (ν_{max} 3530 cm^{-1}), γ -lactone (ν_{max} 1778 cm^{-1}), ester carbonyl (ν_{max} 1741 cm^{-1}), and α,β -unsaturated ketonic carbonyl (ν_{max} 1685 cm^{-1}) groups. From the ^{13}C NMR (Table 1), HSQC, and HMBC spectra, an α,β -unsaturated ketone was deduced from the signals of three carbon signals at δ_C 202.6 (C-12), 125.9 (CH-13), and 154.6 (CH-14). The presence of an exocyclic olefin was confirmed by the signal of an sp^2 methylene carbon at δ_C 119.8 (CH₂-16), and further supported by two olefin proton signals at δ_H 5.69 (1H, ddd, $J = 2.4, 2.4, 1.8$ Hz, H-16a) and 5.37 (1H, br s, H-16b) in the 1H NMR spectrum (Table 1). In addition, three carbonyl resonances at δ_C 176.2 (C-19), 170.2, and 169.5 ($2 \times$ ester carbonyls), confirmed the presence of a γ -lactone and two ester groups; two acetate methyls (δ_H 2.25 and 2.15, each 3H \times s; δ_C 21.1 and 21.7, Me \times 2) were observed. Based on the ^{13}C NMR and numbers of unsaturation, **1** was established as a tricyclic diterpenoid.

The gross structure of **1** was verified by 2D NMR studies. ^1H NMR coupling information in the COSY spectrum enabled identification of C2-C3-C4, C6-C7, C9-C10-C11-C20, C13-C14, and C17-C18 units (Figure 2). These data, together with the 2J - or 3J - ^1H - ^{13}C long-range correlations observed in an HMBC experiment, established the connectivities from C-1 to C-14 (Figure 2). An exocyclic carbon-carbon double bond attached at C-5 was confirmed by an HMBC between H₂-16/C-6. The ring junction C-15 methyl group was positioned at C-1 from an HMBC between H₃-15/C-1, C-2, C-10, and C-14. A hydroxy group at C-8 was to infer that an HMBC of a hydroxy proton at δ_{H} 3.43 (1H, s, OH-8) to C-8 and C-9. The presence of an acetoxy group at C-9 was confirmed by an HMBC from δ_{H} 5.12 (H-9) to the acetate carbonyl at δ_{C} 170.2. Six of the eight oxygen atoms in the molecular formula of **1** could be accounted for the presence of one α,β -unsaturated ketone, one γ -lactone, one ester, and a hydroxy group. Thus, the remaining two oxygen atoms had to be positioned at C-2 as an acetoxy group, as indicated by its ^1H and ^{13}C NMR chemical shifts (δ_{H} 4.82, 1H, d, $J = 8.4$ Hz; δ_{C} 79.2, CH-2), although no HMBC was observed between H-2 to any acetate carbonyl carbon.

The intensity of sodiated molecule $[\text{M} + 2 + \text{Na}]^+$ isotope peak observed in ESIMS $[(\text{M} + \text{Na})^+:(\text{M} + 2 + \text{Na})^+ = 3:1]$ was strong evidence of the presence of a chlorine atom in **1**. The methine unit at δ_{C} 67.2 was correlated to the methine proton at δ_{H} 4.84 in the HSQC spectrum. The latter methine signal was 3J -correlated with H-7 (δ_{H} 5.78), proving the attachment of a chlorine atom at C-6.

Table 1. ^1H (600 MHz) and ^{13}C (150 MHz) NMR (in CDCl_3) data for briaranes **1** and **2**

C/H	1		2	
	δ_{H} (J in Hz)	δ_{C} , ^a type	δ_{H} (J in Hz)	δ_{C} , ^a type
1		44.7, C		38.1, C
2	4.82 d (8.4)	79.2, CH	5.14 d (9.6)	75.0, CH
3 α / β	1.88 m; 2.39 m	28.3, CH ₂	3.39 dd (9.6, 4.2)	60.3, CH
4 α / β	2.58 m; 1.63 m	27.8, CH ₂	3.59 d (4.2)	57.1, CH
5		n. o. ^b		n. o. ^b
6	4.84 br s	67.2, CH	5.36 ddd (3.6, 3.0, 3.0)	n. o. ^b
7	5.78 br s	78.1, CH	5.02 d (3.6)	76.5, CH
8		82.8, C		84.0, C
9	5.12 d (4.8)	74.3, CH	5.35 d (8.4)	69.4, CH
10	2.99 dd (4.8, 4.8)	38.4, CH	1.75 dd (8.4, 1.8)	37.4, CH
11	2.63 qd (7.2, 4.8)	46.6, CH	2.28 qdd (7.2, 4.8, 1.8)	36.0, CH
12		202.6, C	4.64 d (4.8)	71.5, CH
13	5.98 d (10.2)	125.9, CH	3.12 d (3.6)	56.7, CH
14	6.19 d (10.2)	154.6, CH	2.89 d (3.6)	61.5, CH
15	1.16 s	18.9, Me	1.22 s	16.5, Me
16a/b	5.69 ddd (2.4, 2.4, 1.8); 5.37 br s	119.8, CH ₂	6.13 d (2.4); 6.04 d (2.4)	121.1, CH ₂
17	2.44 q (7.8)	42.1, CH	2.44 q (7.2)	45.4, CH
18	1.29 d (7.8)	9.9, Me	1.18 d (7.2)	6.2, Me
19		176.2, C		173.8, C

20	1.32 d (7.2)	15.0, Me	1.03 d (7.2)	9.5, Me
OH-8	3.43 s			
OAc-2		169.5, C		169.0, C
	2.25 s	21.1, Me	2.14 s	20.9, Me
OAc-9		170.2, C		169.5, C
	2.15 s	21.7, Me	2.22 s	22.0, Me
<i>n</i> -OC(O)Pr-12				172.3, C
			2.33 t (7.2)	36.0, CH ₂
			1.67 sext (7.2)	18.5, CH ₂
			0.95 t (7.2)	13.6, Me

^a Due to the absence of signals, the ¹³C chemical shifts were assigned by the assistance of HSQC and HMBC spectra. ^b n. o. = not observed.

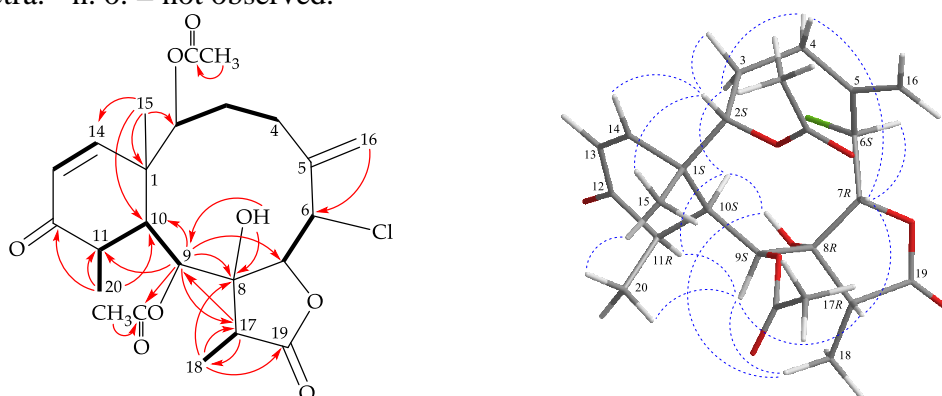


Figure 2. The COSY (—), selective HMBC (↷), and key NOESY (⋯) correlations of **1**

The relative configuration of **1** was determined by correlations observed in a NOESY experiment (Figure 2). Naturally occurring briaranes have β -face of Me-15 at C-1 and α -orientation of H-10, which was proved by the lack of an NOE effect between H-10 and H₃-15. The NOE correlation between H-10/H-11, H-10/H-3 α , H-3 α /H-4 α , H-10/OH-8, and OH-8/H₃-18 demonstrated that all of these groups were α -oriented, and correlations of H-4 β /H-7, H-6/H-7, and H-7/H-17 indicated β -disposition for these groups. The *cis* geometry of the C-13/14 double bond was indicated by a 10.2 Hz coupling constant between H-13 and H-14. H-9 was found to correlate with H-11, H-17, and H₃-20. From a consideration of molecular model, H-9 was found to be reasonably close to H-11, H-17, and H₃-20, thus, H-9 should be placed on the α face, and H-17 was β -oriented in the γ -lactone moiety. Furthermore, H-2 correlated with H-14, H₃-15, and H-3 β , suggested that this proton should be α -oriented at C-2 by modeling analysis. As briaranes **1–4** were isolated along with **5** and **6** from the same target organism, it is reasonable on biogenetic grounds to assume that **1–4** have the same absolute configurations as those of **5** and **6**. Therefore, the configurations of the stereogenic carbons of **1** were determined as 1*S*,2*S*,6*S*,7*R*,8*R*,9*S*,10*S*,11*R*, and 17*R*.

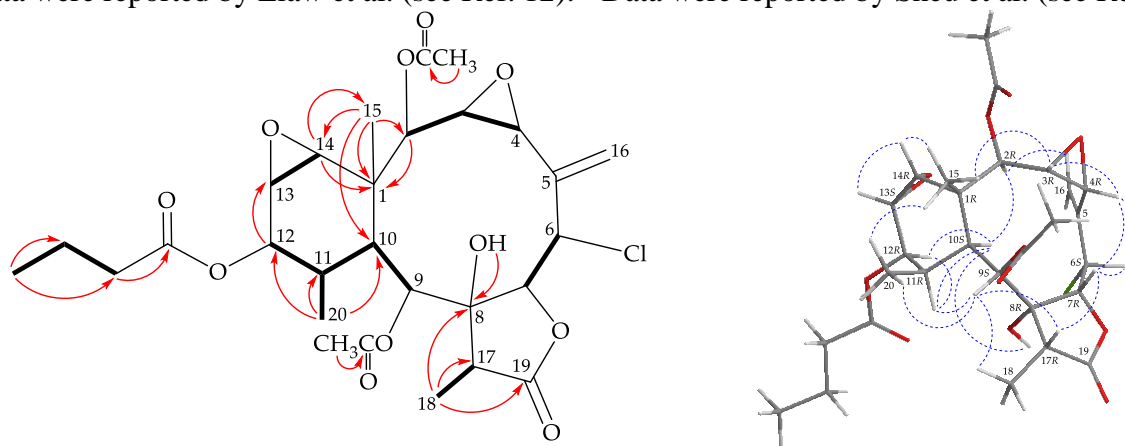
In a previous study, the structure of **1** as we presented in this paper had been reported and was claimed to be tentative.¹⁴ However, there is not any spectroscopic data, related to this compound were reported in later study. Because the structure of **1** has been established by extensive spectroscopic methods in this study. The authors suggested that the structure of **1** shown in ref.14 should be re-examined.

Briarane **2** (briarenol N) was found to have a molecular formula of $C_{28}H_{37}ClO_{11}$ based on its HRESIMS at m/z 607.19172 (Calcd for $C_{28}H_{37}^{35}ClO_{11} + Na$, 607.19166). Its absorption peaks in the IR spectrum showed ester carbonyl, γ -lactone, and broad OH stretching at 1740, 1784, and 3447 cm^{-1} , respectively. The ^{13}C NMR spectrum indicated that three esters and a γ -lactone were present, as carbonyl resonances were observed at δ_C 169.0, 169.5, 172.3, and 173.8. The 1H NMR spectrum also indicated the presence of two acetate methyls (δ_H 2.14 and 2.22, both 3H \times s) (Table 1). The additional acyl group was found to be an *n*-butyroxyl group based on the 1H NMR studies, including an 1H - 1H COSY experiment (Figure 3), which revealed seven contiguous protons (δ_H 0.95, 3H, t, $J = 7.2$ Hz; 1.67, 2H, sext, $J = 7.2$ Hz; 2.33, 2H, t, $J = 7.2$ Hz). The carbon signal at δ_C 172.3 was correlated with the signals of the methylene protons of *n*-butyrate at δ_H 2.33 in the HMBC spectrum (Figure 3), and was consequently assigned as the carbon atom of the *n*-butyrate carbonyl. From the COSY experiment, it was possible to establish the separate spin systems from H-2/H-3/H-4, H-6/H-7, H-9/H-10/H-11/H-12, H-13/H-14, and H-11/H₃-20. These data, together with the correlations observed in the HMBC experiment, suggested the briarane molecular framework of **2**. It was found that the 1H and ^{13}C NMR chemical shifts of **2** resembled those of known briarane analogues, briaviolide E (**7**)¹² and briaexcavtolide E (**8**)¹³ (Chart 1), except that the signals corresponding to the isovaleroxy group in **7**; and one of the acetoxy groups in **8**, were replaced by signals for an *n*-butyroxyl group in **2**. However, due to no HMBC detected between H-2, H-9, and H-12 and ester carbonyls, the positions of *n*-butyroxyl and acetoxy groups in **2** cannot be determined by HMBC. By comparison of the proton and ^{13}C chemical shifts for oxymethines C-2, C-9, and C-12; and the NMR chemical shifts for the acyloxy groups at these positions (C-2, C-9, and C-12) among briaranes **2**, **7**, and **8**, it was found only the data of C-12 oxymethine in **8** were different from those of **2** and **7** (Table 2). Based on the above observations, the *n*-butyrate ester in **2** was identified as being attached at C-12, and the remaining acetoxy groups were positioned at C-2 and C-9, respectively. Locations of the other functional groups were confirmed by other HMBC and COSY correlations (Figure 3), and hence briarenol N was assigned as the structure of **2**, and the configurations of the stereogenic carbons were elucidated as 1*R*,2*R*,3*R*,4*R*,6*S*,7*R*,8*R*, 9*S*,10*S*,11*R*,12*R*,13*S*,14*R*, and 17*R* (Figure 3).

Table 2. Key ^1H (400 MHz, CDCl_3) and ^{13}C (100 MHz, CDCl_3) NMR data for briaranes **2**, **7**, and **8**

C/H	2		7^a		8^b	
	δ_{H} (<i>J</i> in Hz)	δ_{C} , type	δ_{H} (<i>J</i> in Hz)	δ_{C} , type	δ_{H} (<i>J</i> in Hz)	δ_{C} , type
2	5.14 d (9.6)	75.0, CH	5.13 d (9.3)	74.9, CH	5.13 d (9.2)	74.9, CH
9	5.35 d (8.4)	69.4, CH	5.32 m	69.4, CH	5.34 d (8.8)	69.3, CH
12	4.64 d (4.8)	71.5, CH	4.64 d (4.8)	71.4, CH	4.61 d (4.8)	71.7, CH
OAc-2		169.0, C		169.0, C		169.0, C
	2.14 s	20.9, Me	2.12 s	20.9, Me	2.14 s	21.0, Me
OAc-9		169.5, C		169.5, C		169.5, C
	2.22 s	22.0, Me	2.19 s	21.9, Me	2.22 s	22.0, Me
OAc-12						168.8, C
					2.10 s	21.0, Me
<i>n</i> -OC(O)Pr-12		172.3, C				
	2.33 t (7.2)	36.0, CH_2				
	1.67 sext (7.2)	18.5, CH_2				
	0.95 t (7.2)	13.6, Me				
Isovalerate-12				171.9, C		
			2.20 m	43.2, CH_2		
			2.10 m	25.7, CH		
			0.96 d (6.3)	22.3, Me		
			0.96 d (6.3)	22.3, Me		

^a Data were reported by Liaw et al. (see Ref. 12). ^b Data were reported by Sheu et al. (see Ref. 13).

**Figure 3.** The COSY (—), selective HMBC (↷), and key NOESY (⋯) correlations of **2**

Compounds **3–6** were identified as solenolide E,⁸ briarenolide R,⁹ excavatolide A,^{10–12} and briaexcavatolide F,¹³ respectively (Chart 1), by comparison of their ^1H and ^{13}C NMR data, and rotation values with those of in the literature.

In *in vitro* anti-inflammatory activity assay, it was found that briarenol N (**2**) showed weak inhibitory effects on the generation of superoxide anions and the release of elastase (inhibition rates = 18.31 and 16.43%, respectively) and excavatolide A (**5**) displayed a weak inhibitory effect in term of reducing the expression of elastase (inhibition rate = 18.77%) by human neutrophils at a concentration of 10 μM , respectively. The rest compounds **1**, **3**, and **4** were inactive (Table 2). Most briaranes are introduced into

the bloodstream where they instantly encounter a complex environment of proteins and phagocytic cells as neutrophils that protect the body against infections. We therefore examined the release of reactive oxygens species (ROS) and elastase by neutrophils after incubation with briaranes **1–5** to estate their immunotoxicity. The lack of significant induction of ROS or increase in the level of elastase supported the low toxicity of **1**, **3**, and **4**.

Table 2. Inhibitory effects of briaranes **1–5** on superoxide anion generation and elastase release by human neutrophils in response to fMLP/CB

Compound	Superoxide Anions	Elastase
	Inh%	
1	1.85 ± 2.51	6.19 ± 6.49
2	18.31 ± 1.39 ***	16.43 ± 2.71 **
3	9.52 ± 3.37 *	2.07 ± 1.71
4	4.98 ± 4.46	−1.06 ± 2.04
5	2.13 ± 4.20	18.77 ± 5.41 *

Percentage of inhibition (Inh%) at 10 μM concentration. Results are presented as means ± S.E.M. ($n = 3$).

* $P < 0.05$, ** $P < 0.01$, *** $P < 0.001$ compared with the control (fMLP/CB) or basal (solvent, DMSO).

EXPERIMENTAL

General Experimental Procedures. NMR spectra were recorded on a 600 MHz JEOL NMR (model ECZ 600 R) or on a 400 MHz JEOL NMR (model ECZ 400 S) spectrometers using the residual CHCl_3 signal (δ_{H} 7.26 ppm) and CDCl_3 (δ_{C} 77.1 ppm) as internal references for ^1H and ^{13}C NMR, respectively. ESIMS and HRESIMS were obtained from the Bruker mass spectrometer with 7 Tesla magnets (model: SolariX FTMS system). Column chromatography, HPLC, IR spectra, and optical rotation were performed according to our earlier research.¹⁵

Animal Material. Specimens of *Briareum excavatum* used for this study were collected from the culturing tank in the NMMBA at April 2016. A voucher specimen was deposited in the NMMBA (voucher no.: NMMBA-TW-GC-2016-031). Identification of the species of this organism was performed by comparison as described in previous studies.^{1–4}

Extraction and Isolation. Sliced bodies (wet/dry weight = 3980/1860 g) of the coral specimen were prepared and extracted with a 1:1 mixture of methanol (MeOH) and dichloromethane (CH_2Cl_2) (1:1) to give a crude extract (104 g). The extract was then applied to a silica gel column chromatograph (C.C.) and eluted with gradients of hexanes/EtOAc (stepwise from 50:1 to 1:2) to furnish fractions A–L. Fractions H and I were combined (19.0 g) and separated on silica gel C.C. using hexanes/EtOAc (stepwise from 50:1 to pure EtOAc) to obtain fractions H1–H8, including compound **5** (38.0 mg, fraction H5). Fraction H6 was chromatographed with silica gel C.C. using hexanes/EtOAc/acetone to obtain

fractions H6A–H6K. Fraction H6E was separated by silica gel C.C. using a mixture of CH₂Cl₂ and acetone (4:1) to obtain fractions H6E1–H6E6. Fraction H6E2 was repurified by NP-HPLC using a mixture of CH₂Cl₂ and acetone (8:1; at a flow rate = 2.0 mL/min) to yield fractions H6E2A–H6E2E, including compound **3** (22.2 mg, fraction H6E2B). Fraction H6E2A was purified by RP-HPLC using a mixture of MeOH and H₂O (70:30; at a flow rate = 4.0 mL/min) to afford **1** (0.2 mg) and **2** (0.1 mg), respectively. Fraction H6G was re-separated by reverse-phase Si C-18 column, using a mixture of acetonitrile and H₂O (1:1) to obtain fractions H6G1–H6G4. Fraction H6G3 was separated by NP-HPLC using a mixture of CH₂Cl₂ and acetone (5:1) to obtain fractions H6G3A–H6G3D. Fraction H6G3C was separated by NP-HPLC using a mixture of CH₂Cl₂ and acetone (4:1; at a flow rate = 1.0 mL/min) to obtain **6** (5.2 mg). Fraction H6K was separated by NP-HPLC using a mixture of *n*-hexane/acetone (10:1) to yield fractions H6K1–H6K4. Fraction H6K4 was purified by RP-HPLC using a mixture of MeOH and H₂O (65:35; at a flow rate = 4.0 mL/min) to afford **4** (0.9 mg).

Briarenol M (1): amorphous powder; $[\alpha]_D^{25} +6$ (*c* 0.07, CHCl₃); IR (KBr) ν_{\max} 3530, 1778, 1741, 1685 cm⁻¹; ¹H (600 MHz, CDCl₃) and ¹³C (150 MHz, CDCl₃) NMR data, see Table 1; ESIMS *m/z* 505 (M + Na)⁺, 507 (M + 2 + Na)⁺; HRESIMS *m/z* 505.15993 (Calcd for C₂₄H₃₁³⁵ClO₈ + Na, 505.15997).

Briarenol N (2): amorphous powder; $[\alpha]_D^{25} -12$ (*c* 0.03, CHCl₃); IR (KBr) ν_{\max} 3447, 1784, 1740 cm⁻¹; ¹H (600 MHz, CDCl₃) and ¹³C (150 MHz, CDCl₃) NMR data, see Table 1; ESIMS *m/z* 607 (M + Na)⁺, 609 (M + 2 + Na)⁺; HRESIMS *m/z* 607.19172 (Calcd for C₂₈H₃₇³⁵ClO₁₁ + Na, 607.19166).

Solenolide E (3): amorphous powder; $[\alpha]_D^{26} +13$ (*c* 0.73, CHCl₃) (ref.⁸ $[\alpha]_D^{20} +11$ (*c* 0.5, CHCl₃)); IR (KBr) ν_{\max} 3486, 1771, 1742, 1682 cm⁻¹; ¹H (400 MHz, CDCl₃) and ¹³C (100 MHz, CDCl₃) NMR data were found to be in agreement with previous study;⁸ ESIMS *m/z* 463 (M + Na)⁺, 465 (M + 2 + Na)⁺.

Briarenolide R (4): amorphous powder; $[\alpha]_D^{25} -2$ (*c* 0.30, CHCl₃) (ref.⁹ $[\alpha]_D^{25} -1$ (*c* 0.2, CHCl₃)); IR (ATR) ν_{\max} 3278, 1773, 1755, 1674 cm⁻¹; ¹H (400 MHz, CDCl₃) and ¹³C (100 MHz, CDCl₃) NMR data were found to be in agreement with previous study;⁹ ESIMS *m/z* 421 (M + Na)⁺, 423 (M + 2 + Na)⁺.

Excavatolide A (5): colorless crystals; $[\alpha]_D^{26} +24$ (*c* 1.80, pyridine) (ref.¹⁰ $[\alpha]_D^{28} +38$ (*c* 0.05, pyridine)); IR (KBr) ν_{\max} 3479, 1760, 1732 cm⁻¹; ¹H (400 MHz, pyridine-*d*₅) and ¹³C (100 MHz, pyridine-*d*₅) NMR data were found to be in agreement with previous study.¹⁰

Briaexcavatolide F (6): colorless crystals; $[\alpha]_D^{26} -14$ (*c* 0.11, MeOH) (ref.¹³ $[\alpha]_D^{25} -21$ (*c* 0.1, MeOH)); IR (KBr) ν_{\max} 3384, 1779, 1721 cm⁻¹; ¹H (400 MHz, CDCl₃) and ¹³C (100 MHz, CDCl₃) NMR data were found to be in agreement with previous study.¹³

Single-Crystal X-Ray Crystallography of Excavatolide A (5). Suitable colorless prisms of **5** were obtained from a solution of pyridine. The crystal (0.267 × 0.194 × 0.152 mm³) belongs to the orthorhombic system, space group *P*2₁2₁2 (#18), with *a* = 15.4549(4) Å, *b* = 17.3937(5) Å, *c* = 8.3835(2)

\AA , $V = 2253.63(10) \text{\AA}^3$, $Z = 4$, $D_{\text{calcd}} = 1.423 \text{ Mg/m}^3$, $\lambda (\text{Cu K}\alpha) = 1.54178 \text{\AA}$. Intensity data were measured on a Bruker D8 Venture diffractometer up to θ_{max} of 75.0° . All 12163 reflections were collected. The structure was solved by direct methods and refined by a full-matrix least-squares procedure.^{16,17} The refined structural model converged to a final $R1 = 0.0316$; $wR2 = 0.0823$ for 4580 observed reflections [$I > 2\sigma(I)$] and 311 variable parameters. The absolute configuration was determined by Flack parameter $x = 0.081(4)$.^{18,19} Crystallographic data for the structure of **5** have been deposited with the Cambridge Crystallographic Data Center as supplementary publication number CCDC 1961870. These data can be obtained free of charge via <http://www.ccdc.cam.ac.uk/conts/retrieving.html> (or from the CCDC, 12 Union Road, Cambridge CB2 1EZ, UK; fax: +44 1223 336033; e-mail: deposit@ccdc.cam.ac.uk).

Single-Crystal X-Ray Crystallography of Briaexcavatolide F (6). Suitable colorless prisms of **6** were obtained from a solution of MeOH. The crystal ($0.292 \times 0.153 \times 0.076 \text{ mm}^3$) belongs to the monoclinic system, space group $P2_1$ (#4), with $a = 10.0752(3) \text{\AA}$, $b = 14.8881(4) \text{\AA}$, $c = 18.8489(5) \text{\AA}$, $V = 2809.64(14) \text{\AA}^3$, $Z = 4$, $D_{\text{calcd}} = 1.322 \text{ Mg/m}^3$, $\lambda (\text{Cu K}\alpha) = 1.54178 \text{\AA}$. Intensity data were measured on a Bruker D8 Venture diffractometer up to θ_{max} of 72.5° . All 18324 reflections were collected. The structure was solved by direct methods and refined by a full-matrix least-squares procedure.^{16,17} The refined structural model converged to a final $R1 = 0.0495$; $wR2 = 0.1314$ for 10989 observed reflections [$I > 2\sigma(I)$] and 707 variable parameters. The absolute configuration was determined by Flack parameter $x = 0.055(7)$.^{18,19} Crystallographic data for the structure of **6** have been deposited with the Cambridge Crystallographic Data Center as supplementary publication number CCDC 1982252. These data can be obtained free of charge via <http://www.ccdc.cam.ac.uk/conts/retrieving.html> (or from the CCDC, 12 Union Road, Cambridge CB2 1EZ, UK; fax: +44 1223 336033; e-mail: deposit@ccdc.cam.ac.uk).

Anti-inflammatory Test. Human neutrophils were obtained from healthy human volunteers and were isolated by Ficoll centrifugation and dextran sedimentation. Purified neutrophils were re-suspended in calcium (Ca^{2+})-free Hank's balanced salt solution (HBSS) buffer at pH 7.4, and were maintained at 4°C before use. For superoxide anion generation assay, neutrophils ($6 \times 10^5 \text{ cell/mL}$) were equilibrated in ferricytochrome *c* (0.6 mg/mL) and Ca^{2+} (1 mM) at 37°C for 5 min and incubated with DMSO (0.1%) or tested compounds for another 5 min.²⁰ Cells were activated with formyl-methionyl-leucyl-phenylalanine (fMLF, $0.1 \text{ }\mu\text{M}$) for 10 min after the priming with cytochalasin B (CB, $1 \text{ }\mu\text{g/mL}$) for 3 min. The change in absorbance was monitored continuously at 550 nm with a spectrophotometer (Hitachi U-3010). For elastase release assay, neutrophils ($6 \times 10^5 \text{ cell/mL}$) were equilibrated in MeO-Suc-Ala-Ala-Pro-Val-*p*-nitroanilide ($100 \text{ }\mu\text{M}$) and Ca^{2+} (1 mM) at 37°C for 5 min and incubated with dimethyl sulfoxide (DMSO) (0.1%) or test compounds for another 5 min. Cells were activated with fMLF ($0.1 \text{ }\mu\text{M}$) for 10 min after the priming with CB ($0.5 \text{ }\mu\text{g/mL}$) for 3 min. The change in absorbance

was monitored continuously at 405 nm with a spectrophotometer.²⁰ The results are recorded as the mean \pm SEM of three measurements. The inhibition % was measured at 10 μ M concentration of each compound and IC₅₀ values were estimated from dose-response curves. Statistical analysis using Student's *t*-tests with SigmaPlot (Systat Software, San Jose, CA, USA).

ACKNOWLEDGEMENTS

This research was supported by grants from the National Museum of Marine Biology and Aquarium; the National Dong Hwa University; and the Ministry of Science and Technology, Taiwan (Grant Nos: MOST 106-2320-B-291-001-MY3, 107-2320-B-291-001-MY3, and 107-2320-B-182A-004-MY2) awarded to Ping-Jyun Sung and Liang-Mou Kuo.

REFERENCES AND NOTES

1. F. M. Bayer, *Proc. Biol. Soc. Wash.*, 1981, **94**, 902.
2. Y. Benayahu, M.-S. Jeng, S. Perkol-Finkel, and C.-F. Dai, *Zool. Stud.*, 2004, **43**, 548.
3. Y. Miyazaki and J. D. Reimer, *Zool. Sci.*, 2014, **31**, 692.
4. K. Samimi-Namin and L. P. van Ofwegen, *Zookeys*, 2016, **557**, 1.
5. Y.-H. Chen, H.-K. Chin, B.-R. Peng, Y.-Y. Chen, C.-C. Hu, L.-G. Zheng, T.-H. Huynh, T.-P. Su, Y.-L. Zhang, Z.-H. Wen, T.-L. Hwang, Y.-C. Wu, and P.-J. Sung, *Heterocycles*, 2020, **100**, 857, and previous review articles in this series.
6. W.-C. Wei, P.-J. Sung, C.-Y. Duh, B.-W. Chen, J.-H. Sheu, and N.-S. Yang, *Mar. Drugs*, 2013, **11**, 4083.
7. H.-Y. Yan, *Changhua J. Med.*, 2004, **9**, 1.
8. A. Groweiss, S. A. Look, and W. Fenical, *J. Org. Chem.*, 1988, **53**, 2401.
9. Y.-D. Su, Z.-H. Wen, Y.-C. Wu, L.-S. Fang, Y.-H. Chen, Y.-C. Chang, J.-H. Sheu, and P.-J. Sung, *Tetrahedron*, 2016, **72**, 944.
10. J.-H. Sheu, P.-J. Sung, M.-C. Cheng, H.-Y. Liu, L.-S. Fang, C.-Y. Duh, and M. Y. Chiang, *J. Nat. Prod.*, 1998, **61**, 602.
11. J. H. Kwak, F. J. Schmitz, and G. C. Williams, *J. Nat. Prod.*, 2001, **64**, 754.
12. C.-C. Liaw, Y.-B. Cheng, Y.-S. Lin, Y.-H. Kuo, T.-L. Hwang, and Y.-C. Shen, *Mar. Drugs*, 2014, **12**, 4677.
13. J.-H. Sheu, P.-J. Sung, J.-H. Su, H.-Y. Liu, C.-Y. Duh, and M. Y. Chiang, *Tetrahedron*, 1999, **55**, 14555.
14. C. D. Harvell, W. Fenical, V. Roussis, J. L. Ruesink, C. C. Griggs, and C. H. Greene, *Mar. Ecol. Prog. Ser.*, 1993, **93**, 165. The structure of **1** was presented as B-3 in this article.

15. C.-C. Lin, W.-F. Chen, G.-H. Lee, Z.-H. Wen, L.-S. Fang, Y.-H. Kuo, C.-Y. Lee, and P.-J. Sung, [*Heterocycles*, 2019, **98**, 984.](#)
16. G. M. Sheldrick, [*Acta Cryst.*, 2015, **A71**, 3.](#)
17. G. M. Sheldrick, [*Acta Cryst.*, 2015, **C71**, 3.](#)
18. H. D. Flack, [*Acta Cryst.*, 1983, **A39**, 876.](#)
19. H. D. Flack and G. Bernardinelli, [*Acta Cryst.*, 1999, **A55**, 908.](#)
20. P.-J. Chen, I.-L. Ko, C.-L. Lee, H.-C. Hu, F.-R. Chang, Y.-C. Wu, Y.-L. Leu, C.-C. Wu, C.-Y. Lin, C.-Y. Pan, Y.-F. Tsai, and T.-L. Hwang, [*EBioMedicine*, 2019, **40**, 528.](#)